LITERATURE CITED

1. M. A. Gol'dfel'd, V. N. Zinov'ev, and V. A. Lebiga, "Structure and fluctuation characteristics of a compressible turbulent boundary layer behind a fan of rarefaction waves," Preprint No. 16–85, ITPM Sib. Otd. Akad Nauk SSSR, Novosibirsk (1985).
2. S. A. Gaponov and A. A. Maslov, "Stability of a supersonic boundary layer with a pressure gradient and suction," in: Development of Perturbations in a Boundary layer [in Russian], ITPM Sib. Otd. Akad Nauk SSSR, Novosibirsk (1979).
3. V. I. Lysenko, "Stability characteristics of a supersonic boundary layer and their relationship to the position of the laminar–turbulent transition of the boundary layer," Izv. Sib. Otd. Akad. Nauk SSSR, Ser. Tekh. Nauk, 1, No. 4 (1985).
4. V. I. Lysenko, "Role of the first and second modes of perturbation in the transition of a supersonic boundary layer," Zh. Prikl. Mekh. Tekh. Fiz., No. 6 (1985).
5. S. A. Gaponov and G. V. Petrov, "Stability of a supersonic boundary layer with rotation of the flow," Izv. Sib. Otd. Akad. Nauk SSSR, Ser. Tekh. Nauk, 5, No. 18 (1987).
6. A. D. Kosinov, "Development of artificial perturbations in a supersonic boundary layer," Dissertation, Physicomathematical Sciences, Novosibirsk (1986).
7. A. D. Kosinov, A. A. Maslov, and S. G. Shevel'kov, "Experimental study of the stability of a supersonic boundary layer on a cone," Izv. Sib. Otd. Akad. Nauk SSSR, Ser. Tekh. Nauk, 4, No. 15 (1987).
8. L. M. Mack, "The stability of the compressible laminar boundary layer according to a direct numerical solution," in: Recent Developments in Boundary Layer Research, Pt. 1, AGAR-Dograph 97 (1965).

STUDY OF A THREE-DIMENSIONAL TURBULENT BOUNDARY LAYER WITH ALLOWANCE FOR COUPLED HEAT TRANSFER

V. I. Zinchenko and O. P. Fedorova

UDC 533.526+536.24

This article examines the solution of a problem concerning the heating of a cone with a spherical blunting in a supersonic air flow at angles of attack in the case where the Reynolds numbers are such as to realize different flow regimes. We study the effect of nonisothermality of the surface of the body on the heat flow reaching it in the turbulent boundary layer, and we evaluate the accuracy of conventional approaches based on calculation of heating with a specified coefficient of heat transfer from the gas phase.

1. In accordance with [1, 2], characteristics of coupled heat transfer will be sought from the solution of a system of equations describing the change in the averaged quantities in a three-dimensional boundary layer [3] and the nonsteady unidimensional equation of heat conduction in the skin of a body with corresponding boundary and initial conditions.

The boundary layer on the spherical part of the body was calculated as being axisymmetric in the coordinate system connected with the stagnation point. We then changed over to a semigeodesic coordinate system connected with the symmetry axis of the body. After the introduction of the stream functions f and φ, the system of equations of the three-dimensional boundary layer appears as follows in Dorodnitsyn–Lees coordinates:

$$\frac{\partial}{\partial\bar{\xi}}\left(l\frac{\partial\bar{u}}{\partial\bar{\zeta}}\right)+(\alpha_4 f+\alpha_3\varphi)\frac{\partial\bar{u}}{\partial\bar{\zeta}}=\alpha_1\left(\bar{u}\frac{\partial\bar{u}}{\partial\bar{\xi}}-\frac{\partial f}{\partial\bar{\xi}}\frac{\partial\bar{u}}{\partial\bar{\zeta}}\right)+\alpha_2\left(\bar{\omega}\frac{\partial\bar{u}}{\partial\eta}-\frac{\partial\varphi}{\partial\eta}\frac{\partial\bar{u}}{\partial\bar{\zeta}}\right)+ \tag{1.1}$$

$$+\beta_1\left(\bar{u}^2-\frac{\rho_e}{\rho}\right)+\beta_2\left(\bar{\omega}^2-\frac{\rho_e}{\rho}\right)+\beta_3\left(\overline{u\omega}-\frac{\rho_e}{\rho}\right);$$

$$\frac{\partial}{\partial\bar{\xi}}\left(l\frac{\partial\bar{\omega}}{\partial\bar{\zeta}}\right)+(\alpha_4 f+\alpha_3\varphi)\frac{\partial\bar{\omega}}{\partial\bar{\zeta}}=\alpha_1\left(\bar{u}\frac{\partial\bar{\omega}}{\partial\bar{\xi}}-\frac{\partial f}{\partial\bar{\xi}}\frac{\partial\bar{\omega}}{\partial\bar{\zeta}}\right)+\alpha_2\left(\bar{\omega}\frac{\partial\bar{\omega}}{\partial\eta}-\frac{\partial\varphi}{\partial\eta}\frac{\partial\bar{\omega}}{\partial\bar{\zeta}}\right)+ \tag{1.2}$$

Tomsk. Translated from Zhurnal Prikladnoi Mekhaniki i Tekhnicheskoi Fiziki, No. 3, pp. 118-124, May-June, 1989. Original article submitted July 20, 1987; revision submitted December 8, 1987.

0021-8944/89/3003-0451$12.50

$$+\beta_4\left(\bar{\omega}^2-\frac{\rho_e}{\rho}\right)+\beta_5\left(\overline{u\omega}-\frac{\rho_e}{\rho}\right);$$

$$\frac{\partial}{\partial\zeta}\left\{\frac{l}{\mathrm{Pr}_\Sigma}\frac{\partial g}{\partial\zeta}+\gamma_1 l\left(1-\frac{1}{\mathrm{Pr}_\Sigma}\right)\frac{\partial}{\partial\zeta}\left[\bar{u}^2+\left(\frac{\omega_e}{u_e}\bar{\omega}\right)^2\right]\right\}+(\alpha_4 f+\alpha_3\varphi)\frac{\partial g}{\partial\zeta}= \tag{1.3}$$

$$=\alpha_1\left(\bar{u}\frac{\partial g}{\partial\xi}-\frac{\partial f}{\partial\xi}\frac{\partial g}{\partial\zeta}\right)+\alpha_2\left(\bar{\omega}\frac{\partial g}{\partial\eta}-\frac{\partial\varphi}{\partial\eta}\frac{\partial g}{\partial\zeta}\right).$$

With allowance for the assumption that the process is unidimensional, the nonsteady equation of heat conduction in the body can be written as follows in the orthogonal semigeodesic coordinate system:

$$\pi_\rho\frac{\partial\theta}{\partial\tau}=\frac{1}{H_1 r_1}\frac{\partial}{\partial n_1}\left(H_1 r_1\pi_\lambda\frac{\partial\theta}{\partial n_1}\right). \tag{1.4}$$

The boundary and initial conditions are as follows:

$$\bar{u}(\xi,\eta,\infty)=1,\ \bar{\omega}(\xi,\eta,\infty)=1,\ g(\xi,\eta,\infty)=1; \tag{1.5}$$

$$\bar{u}(\xi,\eta,0)=0,\ \bar{\omega}(\xi,\eta,0)=0,\ f(\xi,\eta,0)=\varphi(\xi,\eta,0)=0, \tag{1.6}$$

$$q_w(\xi,\eta,0)\sqrt{\mathrm{Re}}\,\mathrm{Pr}\frac{\lambda_{e0}}{\lambda_{1*}}-\pi_\sigma\theta_w^4=-\pi_\lambda(\theta_w)\frac{\partial\theta}{\partial n_1}(\tau,0);$$

$$\frac{\partial\theta}{\partial n_1}\left(\tau,\frac{L}{R_N}\right)=0\ \text{ or }\ \theta\left(\tau,\frac{L}{R_N}\right)=\theta_i,\ \theta(0,n_1)=\theta_i. \tag{1.7}$$

Here and below, ξ is the dimensionless length of an arc reckoned from the symmetry axis; η, an angle reckoned from the windward side in the plane of symmetry of the body, rad; $\zeta=u_e r_w\int_0^n\rho\,dn\Big/\left(2R_N\int_0^\xi\rho_e\mu_e u_e r_w^2\,d\xi\right)^{1/2}$ and $n_1=-n/R_N$ are directed along a normal to the outer contour on different sides; $g=H/H_{e0}$, $\bar{u}=\partial f/\partial\zeta$, $\bar{\omega}=\partial/\partial\zeta$, dimensionless enthalpy and velocity components in the longitudinal and circumferential directions; $\alpha_1=\int_0^\xi\rho_e\mu_e u_e r_w^2\,d\xi\Big/\rho_e\mu_e u_e r_w^2$, $\alpha_2=\frac{\omega_e}{u_e\bar{r}_w}\alpha_1$, $\alpha_3=\frac{\alpha_1}{\bar{r}_w}\frac{\partial}{\partial\eta}\left(\frac{\omega_e}{u_e}\right)+\frac{\omega_e}{\rho_e\mu_e u_e^2\bar{r}_w^3}\frac{\partial}{\partial\eta}\left(\int_0^\xi\rho_e\mu_e u_e\bar{r}_w^2 d\xi\right)$, $\alpha_4=1$, $\beta_1=\frac{\alpha_1}{u_e}\frac{\partial u_e}{\partial\xi}$, $\beta_2=-\alpha_1\left(\frac{\omega_e}{u_e}\right)^2\frac{1}{\bar{r}_w}\frac{d\bar{r}_w}{d\xi}$, $\beta_3=\alpha_2\frac{1}{u_e}\frac{\partial u_e}{\partial\eta}$, $\beta_4=\frac{\alpha_2}{\omega_e}\frac{\partial\omega_e}{\partial\eta}$, $\beta_5=\alpha_1\left(\frac{1}{\bar{r}_w}\frac{d\bar{r}_w}{d\xi}+\frac{1}{\omega_e}\frac{\partial\omega_e}{\partial\xi}\right)$; $\bar{r}_w=\frac{r_w}{R_N}$, $\gamma_1=\frac{u_e^2}{2H_{e0}}$, $\pi_\rho=\frac{\rho_1 c_1}{\rho_{1*}c_{1*}}$, $\pi_\lambda=\frac{\lambda_1}{\lambda_{1*}}$, $\pi_\sigma=\frac{\varepsilon\sigma T_*^3}{\lambda_{1*}}$, dimensionless coefficients and parameters; $q_w=\frac{\mu_w}{\mathrm{Pr}}\frac{\partial H}{\partial n}\Big|_w\frac{\sqrt{\mathrm{Re}}}{\rho_{e0}V_m H_{e0}}$, $\theta=\frac{T}{T_{e0}}$, $\tau=\frac{t}{t_*}$, dimensionless heat flux, temperature, and time; $t_*=\frac{R_N^2\rho_{1*}c_{1*}}{\lambda_{1*}}$, $V_m=\sqrt{2H_{e0}}$, R_N, L, characteristic times and the velocity, radius of blunting, and thickness of the skin; $H_1=1-kn$, $r_1=\bar{r}_w-n_1\cos\beta$, the Lamé constants ($k$ is the curvature of the generatrix, β is the angle of inclination of the generatrix to the symmetry axis); the indices e, e0, and w denote values of the external boundary of the boundary layer, while the indices 1, *, and T denote characteristics of the solid phase, characteristic quantities, and characteristics of turbulent transport.

We used a two-layer model of a turbulent boundary layer [4] to describe the turbulent flow. In the internal region, the coefficient of eddy viscosity was determined from the Prandtl formula with a van Dreist–Sebechi damping factor generalized to the three-dimensional case

$$\mu_T=0.16\rho n^2\left\{1-\exp\left(-\frac{n}{A}\right)\right\}^2\left\{\left(\frac{\partial u}{\partial n}\right)^2+\left(\frac{\partial\omega}{\partial n}\right)^2\right\}^{0.5}, \tag{1.8}$$

$$A=26\nu\sqrt{\rho/\tau_w}/(1-11.8\bar{p})^{-0.5},\ \nu=\frac{\mu}{\rho},\ U_e=(u_e^2+\omega_e^2)^{0.5},$$

$$\bar{p}=-\frac{\nu}{\rho_e\left(\frac{\tau_w}{\rho}\right)^{1.5}}\frac{1}{U_e}\left(\frac{u_e}{R_N}\frac{\partial p_e}{\partial\xi}+\frac{\omega_e}{r_w}\frac{\partial p_e}{\partial\eta}\right),$$

$$\tau_w=\mu_w\left[(\partial u/\partial n|_w)^2+(\partial\omega/\partial n|_w)^2\right]^{0.5}.$$

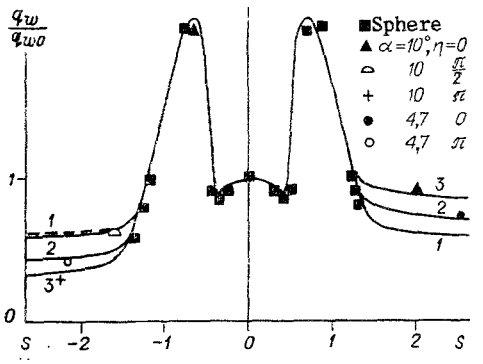

Fig. 1

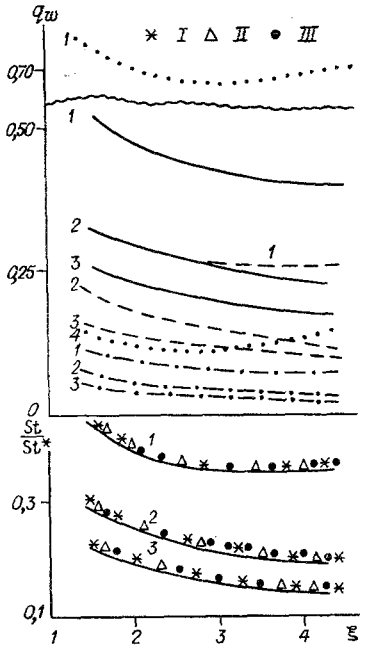

Fig. 2

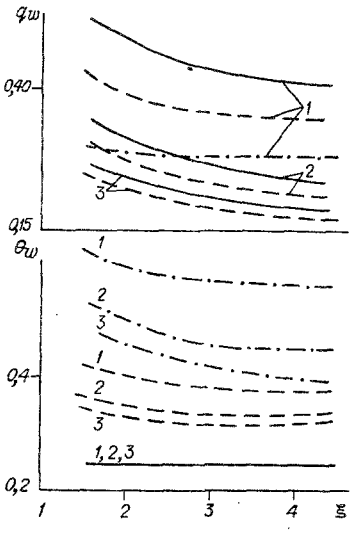

Fig. 3

In the external region, the coefficient of eddy viscosity was calculated from the Clausius formula

$$\mu_T = 0.016\rho\left[1 + 5.5\left(\frac{n}{\delta}\right)^6\right]^{-1}\int_0^\infty [U_e - (u^2 + \omega^2)^{0.5}]\,dn. \qquad (1.9)$$

The boundary between the internal and external regions was found from the condition of equality of the coefficients (1.8) and (1.9).

To calculate flow in the transitional region, we used the formulas

$$l = \frac{\rho\mu}{\rho_e\mu_e} + \Gamma\frac{\rho\mu_T}{\rho_e\mu_e},\quad \mathrm{Pr}_\Sigma = \frac{(\mu + \Gamma\mu_T)\,\mathrm{Pr}\,\mathrm{Pr}_T}{\mu\,\mathrm{Pr}_T + \Gamma\mu_T\,\mathrm{Pr}},$$

where Γ is the coefficient of longitudinal alternation. This coefficient was determined in [5] for the case of flow about bluff bodies. For the laminar flow region, $\Gamma = 0$. For developed turbulence, $\Gamma = 1$. The beginning of the transitional region was determined from the point of loss of stability found on the spherical blunting for the critical value of the Reynolds number

$$\mathrm{Re}^{**} = \frac{u_e\rho_e\delta^{**}}{\mu_e} = 200,\quad \delta^{**} = \int_0^\infty \frac{\rho u}{\rho_e u_e}\left(1 - \frac{u}{u_e}\right)dn.$$

In performing the calculations, we chose the values $Re = V_m\rho_{e0}R_N/\mu_{e0}$ so that the laminar-turbulent transition took place on the spherical part of the body. We used the method in [6] in solving the problem of the development of an axisymmetric boundary layer from the stagnation point, with allowance for the laminar, transitional, and turbulent flow regimes. On the external boundary of the boundary layer, the conditions were chosen on the basis of calculations of inviscid flow about a body [7] and were approximated by means of two-dimensional smoothing splines [8].

The difference schemes for the theoretical regions in the gas phase and the body were obtained by an iterative-interpolational method [9] with an approximation error $O(\Delta\zeta)^2 + O(\Delta\xi) + O(\Delta\eta)$, $O(\Delta n_1)^2 + O(\Delta\tau)$. The integration step was chosen from the condition of the presence of theoretical convergence as determined by the method in [10].

In obtaining the numerical solution for $Pr = 0.72$, $Pr_T = 1$, the coefficient of molecular viscosity μ was assigned by means of Sutherland's formula. The thermophysical characteristics of the material were assumed to be constant, and the following parameters were varied: Re and M_∞, the temperature factor θ_w, the angle of attack α, and the parameter $S = \sqrt{Re\,Pr}\lambda_{e0}/\lambda_{1*}$. The latter parameter is used in problems of coupled heat transfer.

2. Let us examine the results of the solution of boundary-value problem (1.1)-(1.3), (1.5), (1.6) in the case of a prescribed surface temperature.

Figure 1 (α = 0, 4.7, 10° for lines 1-3) shows the dependence of the relative heat flux q_w/q_{w0} on the coordinate s (reckoned from the stagnation point) in the plane of symmetry of the flow. These results were obtained in the solution of the problem of a three-dimensional turbulent boundary layer for the data in [11] ($M_\infty = 5$, $\beta = 9°$, $Re = 5.03\cdot10^6$, $\theta_w = 0.25$). The positive values of s correspond to the windward side, while the negative values correspond to the lee side. The symbols denote the results of the experimental study in [11], the dashed curve shows the theoretical dependence of q_w/q_{w0} on s for $\alpha = 10°$ along the meridional section $\eta = \pi/2$. The heat flows for $\eta = \pi/2$ are close to the flows realized in the case of axisymmetric flow about the same cone. This result has to do with the weak effect of divergence of the streamlines at the meridian $\eta = \pi/2$ on the local heat losses and is consistent with the experimental results for both the turbulent and laminar flow regimes. The satisfactory agreement between the theoretical and experimental data on heat flux is evident from Fig. 1, thus lending validity to the turbulent boundary-layer model being used here.

An increase in the angle of attack on the windward side is accompanied by an increase in heat flux, while an increase in the angle on the lee side is accompanied by a reduction in heat flux. A further increase in the angle of attack may be accompanied by the appearance of a local pressure maximum $p_e(\eta)$ with $\eta = \pi$, leading to restructuring of the flow inside the boundary layer and the formation of a spreading region. As a result, the thickness of the boundary layer decreases on the lee side and heat flux begins to increase.

Such behavior of $q_w(\xi)$ is seen on the lee side at $\alpha = 20.9°$ (Fig. 2). In Fig. 2, dashed curves 1 and 4 correspond to $\eta = 0$, π, respectively, while $\theta_w = 0.05$. Experimental studies [11] showed that for $\alpha = 20.9°$ the heat fluxes at $\eta = \pi$ also behave nonmonotonically. It should be noted that the theoretical data on pressure p_e on the lee side for this angle of attack agrees satisfactorily at $\xi \leq 5$ with the distribution of p_e obtained empirically in [11]. The nonmonotonic behavior of the function $q_w(\xi)$ (dashed line 1, Fig. 2) at $\eta = 0$ for $\alpha = 20.9°$ is due to the increase in pressure at $\xi \geq 2.7$ for the given α.

Let us examine the effect of the temperature factor on the heat fluxes q_w and the ratio of the Stanton numbers St/St^*, where $St^* = q_w^*/[\rho_\infty V_\infty c_p(T_{e0} - T_w^*)]$ corresponds to the maximum value of heat flux q_w^* reached in the neighborhood of the Mach line of the sphere. For the governing parameters shown in Fig. 1, Fig. 2 shows the relations $q_w(\xi, \eta)$ and $St/St^*(\xi, \eta)$ in the meridional sections $\eta = 0$, $\pi/2$, 2.2 with $\alpha = 10°$ (curves 1-3). Here, the solid lines correspond to the value $\theta_w = 0.248$, the dashed lines correspond to $\theta_w = 0.5$, and the dot–dash lines correspond to laminar flow at $\theta_w = 0.248$. It is evident that for these flow conditions the heat fluxes depend appreciably on the temperature factor and that $q_w(\xi, \eta)$ is 4-5 times greater in the turbulent regime than in the laminar regime.

The values of St/St^* change only slightly with a change in the temperature factor by an order of magnitude. Points I and II show St/St^* for $\theta_w = 0.05$ and 0.248 in all sections η (relations 1-3). The solid line corresponds to $\theta_w = 0.5$. The conservative behavior of St/St^* makes it possible to construct reliable methods for determining fluxes to an isother-

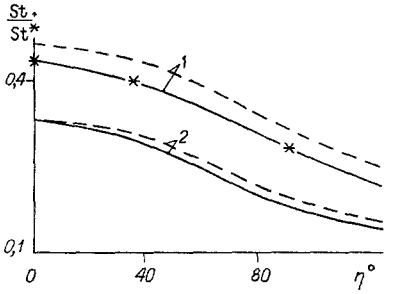

Fig. 4

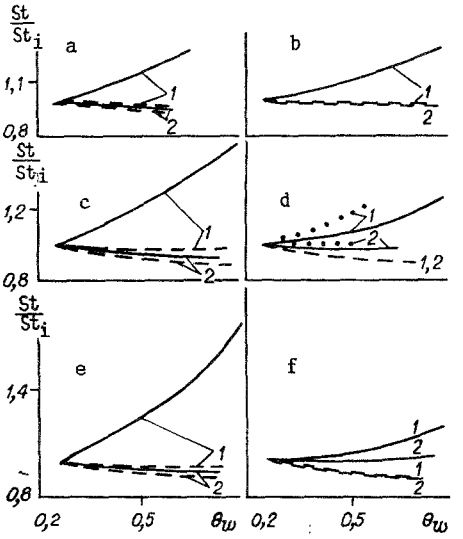

Fig. 5

mal surface. Points III show the distributions of St/St* obtained from the formula in [12]. Our calculations show that an increase in θ_w from 0.05 to 0.8 causes a change in St/St* by no more than 14% over the entire surface of the body.

It follows from Figs. 1 and 2 that the heat-flux distribution on the surface is complex in character, determining $T_w(\xi, \eta)$ and the temperature field inside the body in the solution of the heating problem.

The results of solution of the problem in the coupled formulation are given in Fig. 3. The calculations were performed with $\alpha = 10°$, $\theta_i = 0.248$, $\sqrt{\mathrm{Re}}\,\mathrm{Pr}\,\lambda_{e0}/\lambda_{1*} = 3.19$, $\partial\theta/\partial n_1(\tau$, $L/R_N = 0$, $L/R_N = 0.1$. The rest of the parameters were the same as in Fig. 1. The dependences of q_w and θ_w on ξ are shown in three meridional sections $\eta = 0$, $\pi/2$, 2.2 (lines 1-3) at the moments of time $\tau = 0$, 0.0055, 0.024 (solid, dashed, and dot–dash curves). As might have been expected, the greatest heating is attained on the windward side in the neighborhood of the symmetry plane. Meanwhile, there is a substantial reduction in the temperature θ_w with a change to the lee side of the body. At the same time, the heat flux and temperature in fixed meridional planes change little along the conical surface at $\xi \geq 3.5$ for the theoretical angle of attack.

Figure 4 presents the results of analysis of the solution shown in Fig. 3 in the form of the dependences of $St/St^* = q_w(\xi, \eta)[1 - \theta_w^*]/[1 - \theta_w(\xi, \eta)]q_w^*$ on the variable η in the sections $\xi = 1.45$, 4.54 (lines 1 and 2) for the moments of time $\tau = 0$ and 0.0055 (solid and dashed curves). Here, the asterisks correspond to the formulas in [12] at the initial moment of time $\tau = 0$ for the isothermal surface. It is evident that the nonisothermal character of the surface leads to an increase in the relative Stanton number specifically as a result of the negative values of $\partial\theta_w/\partial\xi$, $\partial\theta_w/\partial\eta$. Meanwhile, the stratification of the curves decreases with movement along the meridional section.

For large periods of time, the attainment of high temperatures on the surface of the spherical blunting causes the heat flow to the region to decrease considerably. In this case, it is better to analyze the solution in the form

$$\frac{St}{St_i} = \frac{q_w(\xi, \eta)\,[1 - \theta_{w.i}(\xi, \eta)]}{q_{wi}(\xi, \eta)\,[1 - \theta_w(\xi, \eta)]},$$

where q_{wi} and θ_{wi} are the heat flux and temperature of the surface at the point (ξ, η) at the initial moment of time. Figure 5 shows the dependence of St/St_i on θ_w obtained in analysis of the solution of the problem of nonsteady heat transfer in the symmetry plane of a blunted cone on the windward side (b, d, f) and lee side (a, c, e) for $\alpha = 5$ (a, b), 10 (c, d), and 20.9° (e, f) in the sections $\xi = 1.45$, 4.54 (lines 1 and 2). The dashed curves show values of St/St_i found in these sections by integration of the equations of a three-dimensional turbulent boundary layer in the neighborhood of the symmetry plane for different isothermal wall temperatures. It is evident that in the solution of the conjugate heat-transfer problem there is a qualitative difference in the behavior of St/St_i in the vicinity of the spherical tip compared to the value found with parametric selection of θ_w.

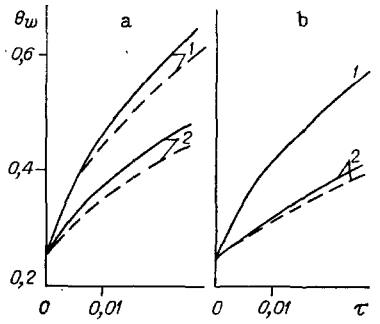

Fig. 6

Such behavior of St/St_i in the solution of boundary-value problem (1.1)-(1.7) is connected with the fact that, as in the axisymmetric case [6], formation of the nonisothermal temperature distribution $[1/(1 - \theta_w)(\partial\theta/\partial\xi) < 0$ causes an increase in the coefficient of heat transfer to the body.

It should be noted that the effect of a nonisothermal distribution of θ_w on the surface can be analyzed qualitatively on the basis of energy conservation equation (1.3). In fact,

$$\left(\frac{\alpha}{c_p}\right) = \frac{\left.\frac{\mu_w}{\mathrm{Pr}_w}\frac{\partial H}{\partial n}\right|_w}{(H_{e0} - H_w)} = \frac{V_m \rho_{e0}}{\sqrt{\mathrm{Re}}} \sqrt{\frac{u_e}{\alpha_1 V_m}\frac{\rho_e}{\rho_{e0}}\frac{\mu_e}{\mu_{e0}}\frac{l_w}{\mathrm{Pr}_w}\left.\frac{\partial \bar{g}}{\partial \bar{\zeta}}\right|_w} \tag{2.1}$$

$[\bar{g} = (g - g_w)/(1 - g_w)]$. After integrating (1.3) in the neighborhood of the symmetry plane, we write the following for Pr = 1 (for example):

$$\left.\frac{l_w}{\mathrm{Pr}_w}\frac{\partial \bar{g}}{\partial \bar{\zeta}}\right|_w = \int_0^\infty (\alpha_4 f + \alpha_3 \varphi)\frac{\partial \bar{g}}{\partial \bar{\zeta}} - \alpha_1 \int_0^\infty \left(\bar{u}\frac{\partial \bar{g}}{\partial \bar{\xi}} - \frac{\partial f}{\partial \bar{\xi}}\frac{\partial \bar{g}}{\partial \bar{\zeta}}\right) d\bar{\zeta} - \\ - \frac{\alpha_1}{1 - g_w}\frac{\partial g_w}{\partial \bar{\xi}} \int_0^\infty \bar{u}(1 - \bar{g})\, d\bar{\zeta}. \tag{2.2}$$

It follows from Eq. (2.2) that the solution is dependent on the quantity $(\alpha_1/1 - g_w)\partial g_w/\partial\xi$, characterizing the nonisothermality of the surface. A detailed analysis of the solution for the laminar flow regime in the boundary layer was presented in [6].

Along with the results in the symmetry plane of the flow, Fig. 5d shows the ratio St/St_i on the lateral conical surface $\eta = 2.2$ (dashed lines). These data were obtained on the basis of the solution of the problem in the coupled formulation in the same sections with respect to ξ. It is evident that nonisothermality of the surface has its greatest effect on the relative Stanton numbers in the neighborhood of the spherical tip and that this effect increases with the transition of η from 0 to π. Also, the difference in the solutions at $\xi = 1.45$ increases with α on the leeward side and decreases with an increase in α on the windward side. This can be attributed mainly to the distance from the stagnation point.

On the section of the conical surface where the flow characteristics change little ($\xi = 4.54$), the values of St/St_i are close the lee side. On the windward side, the stratification of the curves increases with an increase in α.

Since it is time consuming to solve the coupled heat-transfer problem, it is interesting to compare the results obtained with exact and discrete formulations of the problem. Taking advantage of the conservative behavior of St/St^* as a function of isothermal temperature θ_w (see Fig. 2), we assign the heat flow from the gas phase $q_w(\xi, \eta, 0)$ in boundary condition (1.6) in the form $q_w = [St(\xi, \eta)/St^*]\alpha^*[1 - \theta_w(\xi, \eta)]$ [$\alpha^* = q_w^*/(1 - \theta_w^*)$ was approximated from the calculated results]. Figure 6 compares the results of solution of the problem in the coupled formulation (solid curves) and the discrete formulation (dashed curves) at $\alpha = 10°$ (a is the change in surface temperature in relation to time for $\xi = 1.45$, while b is the same for $\xi = 4.54$; lines 1 and 2 correspond to the meridional planes $\eta = 0$, 2.2).

It follows from comparison of the curves $\theta_w(\tau)$ in the regions where the local derivatives $\partial\theta_w/\partial\xi$, $\partial\theta_w/\partial\eta$ are significant that their contribution to the heat-transfer coefficient is important. This results in lowering of the surface temperature in the discrete formulation, when the value of (α/c_p) for isothermal conditions is used. For sections of the conical surface where the flow characteristics change little, the heat-transfer coefficient found for isothermal conditions can be employed. It should be noted that the nonisothermality of θ_w has less effect on the formation of the heat-transfer coefficient in the turbulent flow regime in the boundary layer than in the case of laminar flow.

Thus, the heat flux is determined first of all by the history of the thermal and dynamic boundary layers and, secondly, by the local derivatives of surface temperature with respect to the circumferential and longitudinal coordinates referred to the temperature or enthalpy gradient. Thus, in those cases when the local derivatives are significant either due to the form of the body or due to an abrupt change in boundary conditions, use of the heat-transfer coefficient found for an isothermal wall may lead to errors in the calculation of the temperature field in the material of the skin.

LITERATURE CITED

1. A. V. Lykov, Heat and Mass Transfer. Handbook [in Russian], Énergiya, Moscow (1972).
2. V. I. Zinchenko and E. G. Trofimchuk, "Solution of nonsimilar problems of laminar boundary-layer theory with allowance for coupled heat transfer," Izv. Akad. Nauk SSSR, Mekh. Zhidk. Gaza, No. 4 (1977).
3. Yu. D. Shevelev, Three-Dimensional Problems of Computational Aerohydrodynamics [in Russian], Nauka, Moscow (1986).
4. T. Sebechi, "Calculation of a three-dimensional boundary layer. Infinite cylinder with slip in the presence of a small secondary flow," AIAA J., No. 6 (1974).
5. K. K. Chen and N. A. Thyson, "Extension of Emmons spot theory to flows on blunt bodies," AIAA J., 9, No. 5 (1971).
6. V. I. Zinchenko and E. N. Putyatina, "Solution of problems of coupled heat transfer in flow about bodies of different form," Zh. Prikl. Mekh. Tekh. Fiz., No. 2 (1986).
7. A. V. Antonets, "Calculation of three-dimensional supersonic flow about blunt bodies with generatrix discontinuities with allowance for the equilibrium and frozen states of the gas in the shock layer," Izv. Akad. Nauk SSSR, Mekh. Zhidk. Gaza, No. 2 (1970).
8. Yu. S. Zav'yalov, B. I. Kvasov, and V. L. Miroshnichenko, Spline-Function Methods [in Russian], Nauka, Novosibirsk (1980).
9. A. M. Grishin, V. N. Bertsun, and V. N. Zinchenko, Iterative-Interpolational Methods and Its Applications [in Russian], TGU, Tomsk (1981).
10. F. G. Blottner, "Investigation of some finite-difference techniques for solving the boundary layer equations," Comput. Meth. Appl. Mech. Eng., No. 6 (1975).
11. G. F. Widhopf and R. Hall, "Transitional and turbulent heat-transfer measurements on a yawed blunt conical nosetip," AIAA J., 10, No. 10 (1972).
12. B. A. Zemlyanskii and G. I. Stepanov, "Calculation of heat transfer in the three-dimensional hypersonic flow of air about thin blunt cones," Izv. Akad. Nauk SSSR, Mekh. Zhidk. Gaza, No. 5 (1981).